



Characterization and Temperature-Dependent Adsorption Potential of Hydrothermally Synthesized Manganese Oxide Nanoparticles

Idris Rabi^{1,2}, Taofik Uthman^{1*}, Serdar Surgun¹, Nasar Mansir³¹Innovate Natural Products Research Group, Department of Chemistry, Nile University of Nigeria, Abuja, Nigeria²National Agency for Science and Engineering Infrastructure, Abuja, Nigeria³Department of Chemistry, Faculty of Physical Sciences, Federal University Dutse, Nigeria

ARTICLE INFO

Article history:

Received 10 September 2025

Revised 14 October 2025

Accepted 28 October 2025

Published online 01 January 2026

ABSTRACT

Water pollution usually results from discharge of untreated or partially treated human and industrial waste into water bodies, and nanomaterials are increasingly being recognized as a sustainable alternative remediation approach. The aim of the present study is to determine the structural properties and possible adsorption property of hydrothermally synthesized MnO₂ nanoparticles. The synthesized nanoparticles were characterized using X-ray diffraction, scanning electron microscopy, energy-dispersive X-ray spectroscopy, Brunauer-Emmett-Teller surface area analysis, Fourier-transform infrared spectroscopy and UV-Visible spectroscopy. The nanoparticles primarily exhibited small crystallite sizes, structural disorder, and mostly amorphous material. Manganese was dominant in the nanoparticles as evidenced by surface shape and chemical composition but diminished with rising temperature. The surface area peaked at 110°C and decreased at higher temperatures possibly due to pore collapse and sintering effect, suggesting that annealing temperature had a significant impact on the mesoporous structure. FTIR and UV-Visible data suggest the presence of surface hydroxyl groups evidenced by moisture absorption, an O-Mn-O stretching that promotes hydrogen bonding and bandgap energies that allow for possible visible-light photocatalysis. Incorporating these results with existing research, the adsorption mechanism is expected to include electrostatic interactions controlled by surface charge, chemisorption via redox-active Mn sites, cation exchange regulated by potassium intercalation, and synergistic physisorption. The study also suggests that controlled thermal treatment enhanced adsorption performance as nanoparticles annealed at 90-110°C are expected to exhibit optimal adsorption qualities. Overall, findings from this study offer a starting point for producing efficient MnO₂-based adsorbents capable of removing organic pollutants and heavy metals in aquatic environment.

Copyright: © 2025 Rabi *et al.* This is an open-access article distributed under the terms of the [Creative Commons Attribution License](#), which permits unrestricted use, distribution, and reproduction in any medium, provided the original author and source are credited.

Keywords: Adsorption, Annealing temperature, Manganese dioxide, Nanoparticles, Morphology

Introduction

Nanoparticles (NPs) are natural or synthetic particles of matter with sizes ranging from 1-100 nm which are capable of creating new materials with novel and unique properties. Despite their small size, they have a relatively large surface to volume ratio which is one of the major reasons for their remarkable physicochemical attributes.¹ They exhibit distinctive attributes such electrical, magnetic, and optical activities among others, in contrast to their bulk phase.² In recent years, transition metals and their oxides have attracted widespread use as NPs because of their special physicochemical properties. Metal oxides are the most significant functional materials with excellent properties that are widely used in electronic devices, sensors, batteries and heterogeneous catalysts.^{3,4} Additionally, transition metal oxides occupy a significant position in the field of research due to their unique properties like electronics conductivity, dielectric properties, bandgap energy and high reactivity.⁵

Experimental and theoretical studies have shown that metal oxides can undergo dramatic thermodynamic crossovers in polymorph stability, as a function of both particle size and composition. Small particles generally exhibit large surface area to volume ratio, meaning a bulk metastable phase with low surface energy can become thermodynamically stabilized at the nanoscale.^{6,7}

Among the transition metal oxides, manganese oxide (MnO₂) stands out due to its abundant reserves, high activity, low toxicity and relatively simple preparation process. It is widely used in oxidation catalyst materials, aqueous batteries, supercapacitors, adsorption and other fields.⁸⁻¹⁰ MnO₂ nanoparticles have recently garnered substantial interest due to their diverse applications in catalysis, energy storage, and environmental remediation, particularly in the adsorption of pollutants from aqueous solutions, owing to their high surface area, redox activity, and environmental compatibility.^{11,12} The effectiveness of MnO₂ nanoparticles as adsorbents is significantly influenced by their morphology and phase composition, which dictate the availability of active sites and overall surface reactivity.^{13,14} The ability to control these properties is crucial for optimizing the adsorption performance of MnO₂ nanoparticles in targeted applications.

Several methods have been deployed in the synthesis of nanoparticles. These include green synthesis using plant extracts, hydrothermal synthesis, sol-gel technique, chemical co-precipitation, thermal decomposition, and laser ablation. For instance, Dayak onion extract nanoparticles were prepared using cross-link methods to improve solubility, stability and bioavailability of active substances.¹⁵ However, this was applicable in drug design to increase absorption and reduce digestive tract interference. Furthermore, green synthesis methods,

*Corresponding author. Email: taofik.sunmonu@nileuniversity.edu.ng
Tel: +2348033939464

Citation: Rabi I, Uthman T, Surgun S, Mansir N. Characterization and Temperature-dependent Adsorption Potential of Hydrothermally Synthesized Manganese Oxide Nanoparticles. Trop J Nat Prod Res. 2025; 9(12): 6367 – 6372 <https://doi.org/10.26538/tjnpr/v9i12.60>

leveraging bioactive compounds in plant extracts, enable environmentally friendly production with controlled particle size and surface characteristics, thereby enhancing biocompatibility and reactivity.^{16,17} Hydrothermal and sol-gel techniques offer precise control over morphology and crystallinity thereby influencing surface area and porosity which are critical for adsorptive applications. Gel formation, followed by calcination, produces porous nano-tablets which enhance adsorption sites.¹⁸ Many studies have reported the synthesis of MnOx nanoparticles by combining hydrothermal methods with subsequent doping to enhance adsorption of heavy metals and organic dyes.¹⁹ The resultant nanoparticles often exhibit high surface area, tailored pore size distribution, and abundant surface functional groups, leading to improved removal efficiency, adsorption kinetics, and recyclability. The hydrothermal approach stands out as a flexible and effective method of producing different nanomaterials. It has proven to be effective for creating nanoparticles with controlled particle size through careful adjustment of pH, temperature, pressure, and reaction time.^{20,21} Therefore, the stability of nanoparticles which may not be feasible at high temperatures is assured by the capacity of the method to accept both low-pressure and high-pressure settings depending on the vapor pressure of primary components of the reaction. It also offers a versatile route for synthesizing MnO₂ nanoparticles with controlled morphologies and phases by manipulating reaction parameters such as temperature, pressure, and reactant concentrations.²² Annealing temperature plays a vital role in tuning the crystalline structure, particle size, and surface properties of the synthesized nanoparticles, consequently impacting their adsorption capabilities.²³ The integration of adsorption studies with comprehensive material characterization facilitates the development of predictive models that enable rational design of MnO₂-based adsorbents with tailored properties for specific environmental applications.²⁴ The crystal structure and phase composition of MnO₂ nanoparticles significantly influence their adsorption capacity and selectivity. Different crystalline phases of MnO₂ such as α -MnO₂, β -MnO₂, γ -MnO₂, and δ -MnO₂ exhibit distinct adsorption properties due to their unique tunnel structures and surface characteristics.²⁵ The ability to predict adsorption behavior based on characterization data holds immense value in accelerating the development of adsorbent materials from metal oxides. Therefore, the objective of the present study is to synthesize MnO₂ nanoparticles using hydrothermal technique at different annealing temperatures followed by characterization of their crystal structure, morphology, surface chemistry, surface area, and optical properties. By analyzing these parameters, the study seeks to predict the adsorption potential of MnO₂ nanoparticles. The novelty of this work lies in its unique provision of a detailed framework linking synthesis conditions to the expected adsorption behavior of MnO₂ nanoparticles, thereby offering valuable insights for the design of effective adsorbents in environmental remediation applications.

Materials and Methods

Chemicals/Reagents and equipment

The chemicals/reagents used in the study included potassium permanganate (Kermel Chemical Company, China), manganese sulfate monohydrate (Loba Chemie, India) and hydrogen peroxide (Central Drug House, India) all with 99% purity. The equipment used were analytical balance (M214A, Italy), scanning electron microscope (TM3030Plus, Hitachi, Japan) and Brunauer-Emmett Teller machine (Nova 4200e, USA). The other equipment namely x-ray diffractometer (ARL X'TRA), UV-Visible spectrophotometer (Evolution 220), energy dispersive spectrometer (PRO:X:800-07334) and FTIR spectrometer (Nicolet iS50) are all products of Thermo Fisher Scientific Company, Switzerland.

Synthesis of MnO₂ nanoparticles

MnO₂ nanoparticles were synthesized using hydrothermal technique as described by Gan et al.²⁰ with slight modifications. The first step was the preparation of precursor solution where MnSO₄·H₂O (0.329 g, 0.01 M) and KMnO₄ (0.632 g, 0.01 M) were mixed and dissolved in 250 mL of H₂O₂ solution (1:1 molar ratio of H₂O₂ to distilled water) and stirred

vigorously for 20 minutes using magnetic stirring to form a homogeneous solution. The resulting dark brown gel-like solution was immediately transferred into an autoclave, sealed and heated at varying temperatures of 70°C, 90°C, 110°C, 130°C and 150°C respectively for a period of 2 h in each case. The reactor was then taken out and allowed to cool to room temperature. The resulting brown-black precipitate was filtered off, washed with distilled water three times to remove the excess ions until a neutral pH was attained, and finally dried for 12 hours in an oven at a temperature of 120°C.

Characterization of MnO₂ nanoparticles

The structure of the synthesized MnO₂ nanoparticles was characterized using X-ray diffraction (XRD) technique. The surface morphology and chemical composition of the nanoparticles were determined using scanning electron microscopy (SEM) and energy dispersive X-ray (EDX) spectroscopy. The major functional groups present in the samples were identified using Fourier Transformed Infrared Spectroscopy (FTIR) while the specific surface area and pore size distribution of the synthesized nanoparticles were determined using Brunauer-Emmett Teller (BET) surface area analysis. Finally, the structural and optical properties of the nanoparticles were determined using UV-Visible spectroscopy.

Statistical analysis

Where applicable, data were presented as mean \pm standard deviation of five replicates. Statistical analysis was performed using Statistical Package for Social Sciences (SPSS; version 23.1) software. A p-value of < 0.05 was considered statistically significant.

Results and Discussion

X-Ray diffraction spectra of synthesized MnO₂ nanoparticles

X-Ray diffraction analysis was carried out to examine the crystalline phase of the synthesized manganese dioxide nanoparticles as depicted in Figure 1. The spectra displayed broad humps and well-defined peaks at various 2 θ positions especially between 10° and 50°, which is characteristic of poorly crystalline or nanocrystalline materials. There are some discernible, though still broad, peaks near the 20 positions of 28°, 37° and 56°. These positions are consistent with the standard MnO₂ phases (δ -MnO₂) and the broadness indicates small crystallite sizes or significant structural disorder as confirmed in previous studies.²⁶ Each spectrum is vertically offset for clarity, but the relative intensity of the major features remains similar across all temperature ranges. The spectra remain unchanged across all temperatures (70-150°C), further confirming persistent structural disorder. A similar crystallinity pattern was reported in the green-synthesized MnO₂ using *Punica granatum* peel, with tetragonal phases matching JCPDS standards.²⁶ All samples retain a largely nanocrystalline or amorphous structure, as evidenced by the broad features and lack of distinct, sharp Bragg reflections. Overall, the high structural disorder and abundant surface defect sites indicate that MnO₂ nanoparticles may be suitable for pollutant adsorption.

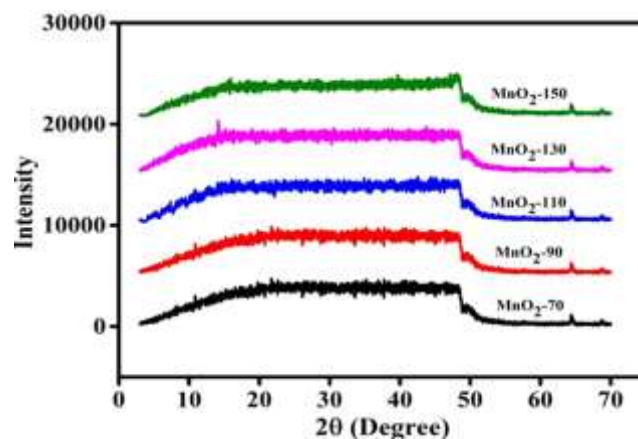


Figure 1: XRD pattern of MnO₂ nanoparticles synthesized at different temperatures

Morphological changes in synthesized MnO₂ nanoparticles

Morphological study of nanoparticles is very important for analyzing their size, shape, and surface, which is directly related to adsorption activity. The morphology of the synthesized MnO₂ nanoparticles as revealed in Figure 2 indicates that they are generally aggregated, forming clusters. At a lower temperature of 70°C, the particles appear finer and more evenly distributed, while at higher temperatures (130°C and 150°C), aggregation became more significant. This suggests a change in texture and possibly particle size aggregation as temperature increases. It has been reported in a previous study that phase transformation in relation to temperature variation in MnO₂ is affected by precursor materials, stoichiometry and particle size.¹⁹ These factors have impacted on the morphology of the synthesized nanoparticles which may influence their adsorptive performance particularly towards heavy metals and dyes. Specifically, tailored morphologies with higher surface area and favorable crystal facets provide more active sites and enhance effective mass transfer, which improve adsorption capacity and kinetics. Consequently, controlling phase transformation and resultant morphology during synthesis is important for optimizing the effectiveness of manganese oxide nanoparticles as adsorbents in wastewater treatment.²⁷

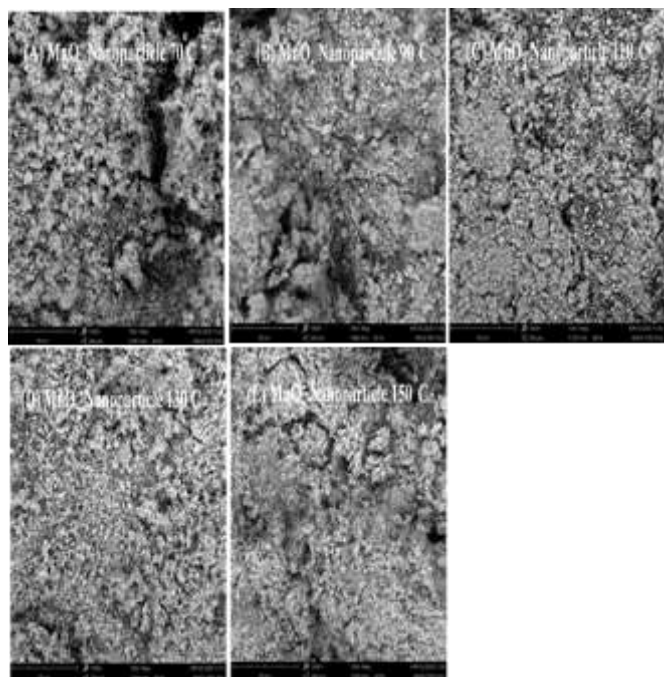


Figure 2: Micrograph of MnO₂ nanoparticles synthesized at different temperatures

Elemental composition of synthesized MnO₂ nanoparticles

Elemental analysis provides information on the component and purity of synthesized materials. The EDX results as presented in Table 1 confirm the presence of manganese (~50-60%) and oxygen (~40-50%) as the dominant primary elements in the synthesized nanoparticles. Other elements such as sulfur, calcium, phosphorus, silicon and aluminum are present as traces of impurities. The presence of potassium may be due to the precursor used in the synthesis (potassium permanganate), which diminishes at higher annealing temperature. Incorporation of potassium into the Birnessite lattice is well known to stabilize the layered structure and facilitate cation exchange mechanisms essential for heavy metal adsorption.¹⁹ The EDX data for MnO₂ nanoparticles revealed that Mn content is relatively high in all samples, indicating successful synthesis. The variations in impurity levels may be attributed to synthesis conditions and washing procedures. For instance, the Mg content is relatively high in the 90°C sample but absent in majority of others. Minor dopants such as sulfur, calcium, and phosphorus may further tailor surface chemistry, potentially affecting adsorption selectivity and affinity through

modification of acidity/basicity.²⁸

Table 1: Weight concentration of elemental component of MnO₂ nanoparticles synthesized at various temperatures

Element	70 °C	90 °C	110 °C	130 °C	150 °C
Manganese	95.46	94.71	96.00	95.95	95.03
Potassium	3.37	2.47	2.03	2.03	2.40
Sulfur	0.50	0.56	0.16	0.15	0.24
Calcium	0.42	0.65	0.27	0.31	0.59
Phosphorus	0.19	0.65	0.97	0.65	0.88
Silicon	0.07	0.26	0.12	0.14	0.25
Aluminum	0.00	0.26	0.46	0.41	0.33
Magnesium	0.00	1.35	0.00	0.00	0.08

Surface area and porosity of synthesized MnO₂ nanoparticles

Trends in surface area and porosity as a function of annealing temperature are presented in Table 2. The data revealed a clear temperature-dependent trend in the surface area and porosity of MnO₂ nanoparticles which are critical parameters for adsorption efficiency. The surface area increased from 235.51 m²/g at 70°C to a peak of 415.41 m²/g at 110°C. This corresponds with increasing pore size and volume indicating enhanced mesoporosity favorable for adsorption through larger accessible surface and facile diffusion pathways.²⁹ However, at 130°C, the surface area dropped sharply, suggesting thermal sintering effect and pore collapse which could negatively affect the adsorption potential of the synthesized nanoparticles.³⁰ The sample at 150°C showed a recovery in surface area, though not exceeding that of the 110°C sample, which suggests stabilization of morphology but not fully restoring optimal adsorption properties. Pore volume followed a similar trend, matching recent findings on temperature-optimized nanomaterial synthesis for catalysis and energy applications.³⁰

Table 2: Surface area and porosity of MnO₂ nanoparticles at different annealing temperatures

Sample	BET Surface area (m ² /g)	Pore Volume (cc/g)	Pore size (cc/g)
MnO ₂ 70°C	235.51 ± 8.55	0.13 ± 0.01	48.25 ± 1.35
MnO ₂ 90°C	342.82 ± 6.32	0.19 ± 0.05	70.47 ± 2.11
MnO ₂ 110°C	415.41 ± 5.43	0.22 ± 0.03	77.99 ± 2.55
MnO ₂ 130°C	142.51 ± 8.29	0.09 ± 0.01	32.34 ± 1.04
MnO ₂ 150°C	355.97 ± 7.49	0.18 ± 0.02	64.80 ± 2.26

UV-Vis spectra of synthesized MnO₂ nanoparticles

The UV-Vis spectra of synthesized MnO₂ nanoparticles showing bandgap values, absorption edge shifts, and their correlation with morphology are presented in Figure 3. A strong absorption peak near 359 nm (bandgap ~3.45 eV) indicates MnO₂ formation. Broader peaks at higher temperatures suggest larger nanoparticles or agglomeration, which reduces electrochemical and surface activities. This is consistent with previous findings which reported that annealing temperature significantly affects optical properties.³¹ The spectra revealed distinct absorption profiles across the UV-visible range (200-800 nm) at different temperatures. The samples exhibited characteristic broad absorption in the UV region with absorption edges extending into the visible range, which is typical for MnO₂ materials. Bandgaps around 1.2-2.0 eV confirm potential photocatalytic activity under visible light, which synergistically improves organic pollutant removal by degrading contaminants adsorbed on nanoparticle surfaces.^{32,33} The spectra revealed clear temperature-dependent variations in both absorption intensity and spectral shape. Samples synthesized at relatively high temperatures exhibited modified absorption profiles, indicating structural and optical property changes upon thermal treatment. It has been confirmed that high annealing temperatures improve grain size and

porosity, which manifest as broader absorption features in UV-Visible spectra.³⁴ The conversion from granular to porous amorphous structure at higher temperatures explains the reduced electrochemical activity and surface reactivity.

FTIR spectra of synthesized MnO₂ nanoparticles

FTIR analysis is known for its high sensitivity, especially in the detection of inorganic and organic species. The FTIR spectra obtained for the synthesized nanoparticles in this study are presented in Figure 4. The spectra showed peaks related to O-Mn-O stretching vibrations (around 520 cm⁻¹), which confirms formation of MnO₂ nanoparticles. Broad O-H (~3400 cm⁻¹) indicates possible surface-adsorbed moisture. The typical Mn-O bond vibrations and surface hydroxyl groups present in the spectra provide active sites for hydrogen bonding and electrostatic interactions that contribute to adsorption affinity.³⁵ The changes in spectra according to the temperature of synthesis may be an indication of alteration in the Mn-O bonding or the presence of impurities.³⁶⁻³⁸ These changes mostly result in creation or modification of surface functional groups such as hydroxyl, oxygen vacancies, and Mn-OH species, which are required for adsorption activity. The presence of these functional groups has the tendency to increase the affinity of MnO₂-based adsorbents towards heavy metals by providing active sites for complexation, ion exchange, and electrostatic interactions. Studies have shown that a high density of surface hydroxyl groups enables binding of heavy metals like lead, cadmium, and chromium, thereby enhancing removal efficiency and selectivity.³⁹ Consequently, oxygen vacancies created during phase transitions or temperature variations serve as reactive centers that promote redox reactions and catalytic degradation of organic contaminants such as dyes in aqueous solutions. Therefore, tuning synthesis parameters to optimize surface chemistry and functional group availability is necessary to maximize the efficiency and effectiveness of MnO₂ nanoparticles in environmental remediation applications.^{19,27}

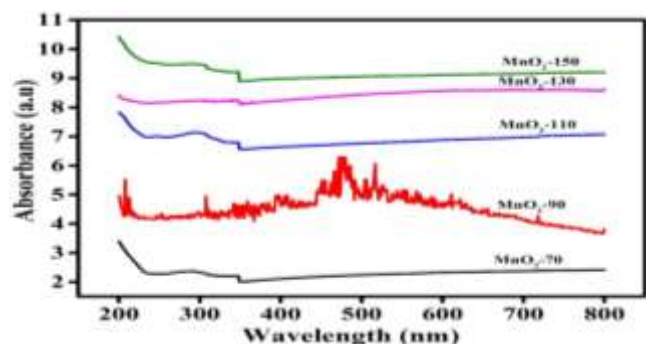


Figure 3: UV- Visible spectra of MnO₂ nanoparticles synthesized different temperatures

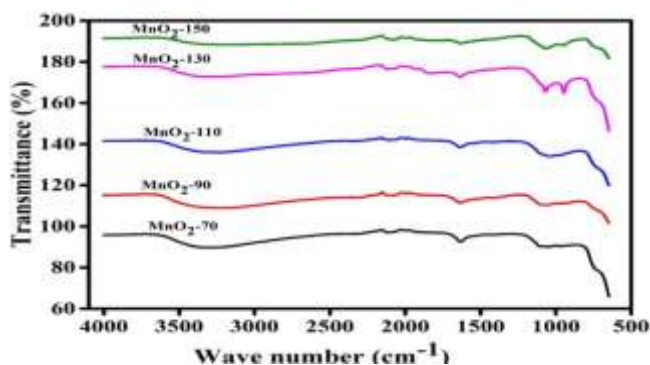


Figure 4: FTIR spectra of MnO₂ nanoparticles at different temperatures

Significant findings from the study

Based on the data obtained from XRD, SEM, EDX, BET, UV-Visible and FTIR spectroscopic analyses, a detailed framework for predicting the adsorption potential of MnO₂ nanoparticles was established. The specific surface area, pore size distribution, and the presence of surface functional groups collectively determine the number of available active sites for adsorption. Bandgap energy and electronic properties influence redox activity and ability to interact with pollutants. By correlating these physicochemical features with synthesis conditions, a predictive model was developed to optimize the synthesis of MnO₂ nanoparticles with tailored adsorption properties. The possible adsorption mechanism of MnO₂ nanoparticles is therefore multifaceted and can proceed by both chemical and physical means.^{32,40} Physisorption, driven by high surface area and mesoporosity, cooperates with chemisorption processes involving redox-active Mn (III/IV) sites and surface hydroxyl functionalities that enable strong binding and possible electron transfer reactions with pollutants.³⁹ Cation exchange and intercalation within the layered structure, modulated by potassium content, may enhance selective heavy metal uptake.⁴¹ Surface charge, influenced by functional groups and annealing induced surface chemistry modification, further governs electrostatic interactions vital for adsorption of ionic species.⁴² Additionally, the adsorption process can be tuned by varying temperature thereby modifying the morphology and surface functional groups. The operation can be achieved by grafting specific groups into the framework or by tuning the net charge based on pH of solution in which the adsorption takes place.⁴³ Carbonaceous nanomaterials can be modified to increase their solubility, reactivity, and adsorptive capacity.⁴⁴ These strategies would enhance the performance of the material in environmental applications.⁴⁵ This is supported by previous studies which reported that nanomaterials with high specific surface area and enhanced adsorption kinetics are particularly suitable for treating wastewater, even at ultralow pollutant concentrations.⁴⁶ Nanostructured materials, including metal oxides, have also been used as adsorbents to remove organic compounds from water.⁴⁷

Conclusion

Hydrothermal synthesis of MnO₂ nanoparticles at different controlled annealing temperatures effectively modified their structural, morphological, and surface chemical properties which directly influence their adsorption potential. The resulting MnO₂ nanoparticles exhibited high structural disorder and abundant surface defect sites, favorable for pollutant adsorption. Potassium content within the layered MnO₂ structure plays a critical role in modulating cation exchange capacity and adsorption selectivity. The study identified 110°C as the optimal annealing temperature yielding maximum surface area and porosity, thereby proposed to facilitate adsorption capacity. At temperatures below and above 110°C, the observed declines in surface characteristics correspond to reduced adsorption potential due to pore collapse or particle sintering. Surface functional groups such as hydroxyls and bandgap-dependent photocatalytic properties further contribute to multifaceted adsorption mechanisms, including redox-active chemisorption and photocatalytic degradation of organic pollutants. These combined effects suggest that MnO₂ nanoparticles synthesized at 90-110°C offer promising adsorbent platforms for the removal of contaminants from aqueous environments. The characterization analysis and theoretical adsorption studies demonstrates the promise of hydrothermally synthesized MnO₂ nanoparticles as effective adsorbents, with annealing temperature serving as a crucial parameter for tailoring their properties for environmental remediation performance. Future prospects for this study should focus on real time application of the synthesized nanoparticles for the removal of organic pollutants and heavy metals in polluted water.

Conflict of Interest

The authors declare no conflict of interest.

Authors' Declaration

The authors hereby declare that the work presented in this article is original and that any liability for claims relating to the content of this article will be borne by them.

References

1. Abdullah M, Alahmari SD, Alharbi FF, Ejaz SR, Waheed MS, Aman S, Al-Sehemi AG, Henaishi AMA, Ahmad Z, Farid HMT. Facile synthesis of MnO₂/g-C₃N₄ for photocatalytic reduction of methylene blue dye under visible light. *J Mater Sci: Mater Electron*. 2024; 35:517. <https://doi.org/10.1007/s10854-024-12166-7>
2. Dhanapal J, Saravanan NS, Jayaprakash NS, Sivakumar NV, Muniasamy NSK, Deivasigamani NV, Shanmugam NB, Sampathkumar NV. Eco-friendly concrete solutions: The role of titanium dioxide nanoparticles in enhancing durability and reducing environmental pollutants-A review. *J Environ Nanotechnol*. 2024;13(3):332-344. Doi: [10.13074/jent.2024.09.243894](https://doi.org/10.13074/jent.2024.09.243894)
3. Nagal V, Tuba T, Kumar V, Alam S, Ahmad A, Hafiz AK, Alshammari MB, Ahmad R. A non-enzymatic electrochemical sensor composed of nano-berries shaped cobalt oxide nanostructures on a glassy carbon electrode for uric acid detection. *New J Chem*. 2022; 46(25): 12333-12341. <https://doi.org/10.1039/d2nj01961b>
4. Alharbi FF, Abdullah M, Aman S, Goudria S, Sadaf A, Abdel T, Taha M, Farid HMT. Development of environmental friendly Mo-doped MnO₂ via hydrothermal route for supercapacitor as pollution-free source of energy. *Appl Phys A*. 2024; 130:236. <https://doi.org/10.1007/s00339-024-07359-0>
5. Yetim NK. Hydrothermal synthesis of Co₃O₄ with different morphology: Investigation of magnetic and electrochemical properties. *J Mol Struct*. 2021; 1226:129414. <https://doi.org/10.1016/j.molstruc.2020.129414>
6. Navrotsky A, Ma C, Lilova K, Birkner N. Nanophase transition metal oxides show large thermodynamically driven shifts in oxidation-reduction equilibria. *Sci*. 2010; 330:199-201. Doi:[10.1126/science.1195875](https://doi.org/10.1126/science.1195875)
7. Navrotsky A. Nanoscale effects on thermodynamics and phase equilibria in oxide systems. *ChemPhysChem*. 2011; 12(12): 2207-2215. <https://doi.org/10.1002/cphc.201100129>
8. Li F, Wang J, Liu L, Qu J, Li Y, Bandari VK, Karnaushenko D, Becker C, Faghih M, Kang T, Baunack S, Zhu M, Zhu F, Schmidt OG. Self-assembled flexible and integratable 3D microtubular asymmetric supercapacitors. *Adv Sci*. 2019; 6(20):1901051 <https://doi.org/10.1002/advs.201901051>
9. Luo S, Xie L, Han F, Wei W, Huang Y, Zhang H, Zhu M Schmidt OG, Wang L. Nanoscale parallel circuitry based on interpenetrating conductive assembly for flexible and high-power zinc ion battery. *Adv Funct Mater*. 2019; 29(28):1901336 <https://doi.org/10.1002/adfm.201901336>
10. Wei H, Wang X, Zhang D, Du W, Sun X, Jiang F, Shi T. Facile synthesis of lotus seedpod-based 3D hollow porous activated carbon/manganese dioxide composite for supercapacitor electrode. *J Electroanal Chem*. 2019; 853:113561. <https://doi.org/10.1016/j.jelechem.2019.113561>
11. Dang TD, Le TTH, Hoang TBT, Mai TT. Synthesis of nanostructured manganese oxides based materials and application for supercapacitor. *Adv Nat Sci Nanosci Nanotechnol*. 2015; 6(2):025011. <https://doi.org/10.1088/2043-6262/6/2/025011>
12. Wei Z, Pashchenko AV., Liedienov N, Zatonovsky IV., Butenko DS, Li Q, Fesich IV, Turchenko V, Zubov E, Polynchuk PY, Pogrebnyak VG, Poroshin VM, Levchenko GG. Multifunctionality of lanthanum-strontium manganite nanopowder. *Phys Chem Chem Phys*. 2020; 22(21):1426. <https://doi.org/10.1039/d0cp01426e>
13. Tuutijärvi T, Lu J, Sillanpää M, Chen G. Adsorption mechanism of arsenate on crystal γ -Fe₂O₃ nanoparticles. *J Environ Eng*. 2010; 136(9): 1943. [https://doi.org/10.1061/\(asce\)ee.1943-7870.0000233](https://doi.org/10.1061/(asce)ee.1943-7870.0000233)
14. Sun M, Lan B, Lin T, Cheng G, Ye F, Yu L, Cheng X, Zheng X. Controlled synthesis of nanostructured manganese oxide: Crystalline evolution and catalytic activities. *Cryst Eng Comm*. 2013; 15: 7010-7018. <https://doi.org/10.1039/c3ce40603b>
15. Annisa R, Lestari RI, Aqila SS, Fanany CT, Fitrianiingsih AA, Rachmawati E, Rahmadiani N, Muti'ah R. Optimisation and characterisation of Dayak onion (*Eleutherine palmifolia* (L.) Merr) extract nanoparticles using cross-link method. *Trop J Nat Prod Res*. 2025; 9(2): 480-486. <https://doi.org/10.26538/tjnpr/v9i2.10>
16. Friday MD. Green synthesis, characterization and applications of manganese oxide nanoparticles. *NanoEra*. 2025; 5(1): 28-41. <https://doi.org/10.5281/zenodo.15729170>
17. Akinniyi JN. Synthesis and characterization of copper nanoparticles using *Allium cepa* (L.) outer peel at ambient temperature. *Trop J Nat Prod Res*. 2025; 9(3): 1144-1149. <https://doi.org/10.26538/tjnpr/v9i3.32>
18. Siddique MAB, Bithi UH, Ahmed AN, Gafur MA, Reaz AH, Roy CK, Islam MM, Firoz SH. Preparation of manganese oxide nanoparticles with enhanced capacitive properties utilizing gel formation method. *ACS Omega*. 2022; 7(51): 5872. Doi:10.1021/acsomega.2c05872
19. Li M, Kuang S, Kang Y, Ma H, Dong J, Guo Z. Recent advances in application of iron-manganese oxide nanomaterials for removal of heavy metals in the aquatic environment. *Sci Total Environ*. 2022; 819: 153157. <https://doi.org/10.1016/j.scitotenv.2022.153157>
20. Gan YX, Jayatissa AH, Yu Z, Chen X, Li M. Hydrothermal synthesis of nanomaterials. *J Nanomater*. 2020; 8917013. <https://doi.org/10.1155/2020/8917013>
21. Schmidt R, Prado-Gonjal J, Moran E. Microwave assisted hydrothermal synthesis of nanoparticles. *Appl Phys*. 2022; 561-572. <https://doi.org/10.48550/arxiv.2203.02394>
22. Raheem ZH, Al Sammarraie AMA. Synthesis of different manganese dioxide nanostructures and studying the enhancement of their electrochemical behavior in zinc-MnO₂ rechargeable batteries by doping with copper. *AIP Conf Proc*. 2020; 2213(1): 020187. <https://doi.org/10.1063/5.0000246>
23. Augustin M, Fenske D, Bardenhagen I, Westphal A, Knipper M, Plaggenborg T, Kolny-Olesiak J, Parisi J. Manganese oxide phases and morphologies: A study on calcination temperature and atmospheric dependence. *Beilstein J Nanotechnol*. 2015; 6(1): 47-59. <https://doi.org/10.3762/bjnano.6.6>
24. Droepenu EK, Wee BS, Chin SF, Kok KY, Maligan MF. Zinc oxide nanoparticles synthesis methods and its effect on morphology: A review. *Biointerface Res Appl Chem*. 2022; 12(3): 4261-4292. <https://doi.org/10.33263/briac123.42614292>
25. Zhao C, Wang B, Theng BKG, Wu P, Liu F, Wang S, Lee X, Chen M, Li L, Zhang X. Formation and mechanisms of nano-metal oxide-biochar composites for pollutants removal: A review. *Sci Total Environ*. 2021; 767:145305. <https://doi.org/10.1016/j.scitotenv.2021.145305>
26. Thilaga-Sundari D, Silambarasan D, Sarika R. Electrochemical performance of manganese dioxide (MnO₂) nanoparticles synthesized by co-precipitation method. *Nanotechnol Perceptions*. 2024; 20(7):3869-3878.
27. Wang R, Gao P, Yuan S, Li Y, Liu Y, Huang C. Precise regulation of the phase transformation for pyrolusite during the reduction roasting process. *Int J Miner Metall Mater*. 2024; 31:81-90. <https://doi.org/10.1007/s12613-023-2688-4>
28. Kumar N, Thorat ST, Reddy KS. Multi biomarker approach to assess manganese and manganese nanoparticles toxicity in *Pangasianodon hypophthalmus*. *Sci Rep*. 2023; 13:8505. <https://doi.org/10.1038/s41598-023-35787-0>
29. Tang SF, Zhou H, Tan WT, Huang JG, Zeng P, Gu JF, Liao B-H. Adsorption characteristics and mechanisms of Fe-Mn oxide modified biochar for Pb(II) in wastewater. *Int J Environ Res Public Health*. 2022;19(14):8420. <https://doi.org/10.3390/ijerph19148420>

30. Xie M, Zhang X, Wang R, Jiao Y, Shu Z, Shan S, Bian Y, Lin H, Chen J, Xu Y. Mn-O bond engineering mitigating Jahn-Teller effects of manganese oxide for aqueous zinc-ion battery applications. *Chem Eng J.* 2024; 494:152908. <https://doi.org/10.1016/j.cej.2024.152908>
31. Namdari T, Astinchap B, Moradian R. Effect of annealing temperature on optical properties, microstructure and surface morphology of manganese dioxide layers. *Optoelectron Adv Mater Rapid Commun.* 2023; 17(3-4):152-158.
32. Wen J, Fang Y, Zeng G. Progress and prospect of adsorptive removal of heavy metal ions from aqueous solution using metal-organic frameworks: A review of studies from the last decade. *Chemosphere.* 2018; 201:627-643. <https://doi.org/10.1016/j.chemosphere.2018.03.047>
33. Xiao L, Deng Y, Zhou H, Lu F, Ke C, Ye Y, Pei X, Xia D, Pan F. Activated carbon fiber mediates efficient activation of peroxymonosulfate systems: Modulation of manganese oxides and cycling of manganese species. *Chinese Chem Lett.* 2023; 34(12):108407. <https://doi.org/10.1016/j.ccl.2023.108407>
34. Falahatgar SS, Ghodsi FE. Annealing temperature effects on the optical properties of MnO₂: Cu nanostructured thin films. *Int J Nanosci Nanotechnol.* 2016; 12(1):7-18.
35. Yao Y, Xu C, Yu S, Zhang D, Wang S. Facile synthesis of Mn₃O₄ reduced graphene oxide hybrids for catalytic decomposition of aqueous organics. *Ind Eng Chem Res.* 2013; 52(10):3637-3645. Doi:10.1021/ie303220x
36. Dessie Y, Tadesse S, Eswaramoorthy R. Physicochemical parameter influences and their optimization on the biosynthesis of MnO₂ nanoparticles using *Vernonia amygdalina* leaf extract. *Arab J Chem.* 2020; 13(8):6472-6492. <https://doi.org/10.1016/j.arabj.2020.06.006>
37. Mekuria AT. Biosynthesis of manganese dioxide nanoparticles and optimization of reaction variables. *J Nanotechnol Nanomater.* 2024; 5(1):31-45.
38. Hassan A, Haris M, Ullah Khan S, Khan I, Akif M, Akhtar N. *Lathyrus aphaca* extract MnO nanoparticles: Synthesis, characterization, and photocatalytic degradation of methylene blue dye. *Photocatal Res Potential.* 2024;1(3):10004. <https://doi.org/10.35534/prp.2024.10004>
39. Zhang H, Zhang Y, Pan Y, Wang F, Sun Y, Wang S, Wang Z, Wu A, Zhang Y. Efficient removal of heavy metal ions from wastewater and fixation of heavy metals in soil by manganese dioxide nanosorbents with tailored hollow mesoporous structure. *Chem Eng J.* 2023; 459:141583. <https://doi.org/10.1016/j.cej.2023.141583>
40. Asghar HMA, Hussain SN, Brown NW, Roberts EPL. Comparative adsorption-regeneration performance for newly developed carbonaceous adsorbent. *J Ind Eng Chem.* 2019; 69:90-98. <https://doi.org/10.1016/j.jiec.2018.09.012>
41. Liu X, Kifle MT, Xie H, Xu L, Luo M, Li Y, Huang Z, Gong Y, Wu Y, Xie C. Biomineralized manganese oxide nanoparticles synergistically relieve tumor hypoxia and activate immune response with radiotherapy in non-small cell lung cancer. *Nanomater.* 2022; 12(18):3138. Doi:10.3390/nano12183138.
42. Pal Singh J, Kumar M, Sharma A, Pandey G, Chae KH, Lee S. Bottom-up and Top-down approaches for MgO. *Sonochemical Reactions.* IntechOpen; 2020. <http://dx.doi.org/10.5772/intechopen.91182>
43. Manousi N, Giannakoudakis DA, Rosenberg E, Zachariadis GA. Extraction of metal ions with metal-organic frameworks. *Mol.* 2019;24(24):1-21. <https://doi.org/10.3390/molecules24244605>
44. Vyas S. Carbonaceous nanomaterials for water pollution remediation: An overview. *EPRA Int J Multidiscip Res.* 2021; 7(1):6185. <https://doi.org/10.36713/epra6185>
45. Ali S, Zahra H, Ahmad MU, Abdel-Rheem AA, Afzaal M, Nawaz R, Abbasi BBK, Irfan A, Jordan YAB. Synergistic photocatalytic and biomedical applications of Ag₂O-immobilized *Bacillus subtilis*-hyaluronic acid. *Microb Cell Fact.* 2025; 24:129. <https://doi.org/10.1186/s12934-025-02750-9>
46. Chenab KK, Sohrabi B, Esrafil M. pH-sensitive organic diimide materials-based superhydrophobic surface for oil-water separation applications. *Mater Res Express.* 2019; 6(12): 125112. Doi:10.1088/2053-1591/ab657b
47. Sousa Neto, VDO, Freire TM, Saraiva GD, Muniz CR, Cunha MS, Fachine PBA, Nascimento RFD. Water treatment devices based on zero-valent metal and metal oxide nanomaterials. In: Nascimento RFD, Ferreira OP, De Paula AJ, Sousa Neto VDO (Eds.). *Nanomaterials applications for environmental matrices.* Elsevier; 2019. 187-225 p. <https://doi.org/10.1016/B978-0-12-814829-7.00005-7>